KLOE Note n^o 189

July 2003

Determination of $\sigma(e^+e^- \to \pi^+\pi^-)$ from radiative processes at DAΦNE

The KLOE Collaboration

A. Aloisio [e], F. Ambrosino [e], A. Antonelli [b], M. Antonelli [b], C. Bacci [j], G. Bencivenni [b], S. Bertolucci [b], C. Bini [h], C. Bloise [b], V. Bocci [h], F. Bossi [b], P. Branchini [j], S. A. Bulychjov [o], R. Caloi [h], P. Campana [b], G. Capon [b], T. Capussela [e], G. Carboni [i], G. Cataldi [d], F. Ceradini [j], F. Cervelli [f], F. Cevenini [e], G. Chiefari [e], P. Ciambrone [b], S. Conetti [m], E. De Lucia [h], P. De Simone [b], G. De Zorzi [h], S. Dell'Agnello [b], A. Denig [c], A. Di Domenico [h], C. Di Donato [e], S. Di Falco [f], B. Di Micco [j], A. Doria [e], M. Dreucci [b], O. Erriquez [a], A. Farilla [j], G. Felici [b], A. Ferrari [j], M. L. Ferrer [b], G. Finocchiaro [b], C. Forti [b], A. Franceschi [b], P. Franzini [h], C. Gatti [h], P. Gauzzi [h], S. Giovannella [b], E. Gorini [d], E. Graziani [j], M. Incagli [f] [1], W. Kluge [c], V. Kulikov [o], F. Lacava [h], G. Lanfranchi [b] J. Lee-Franzini [b,k], D. Leone [h], F. Lu [b,n], M. Martemianov [b], M. Matsyuk [b], W. Mei [b], L. Merola [e], R. Messi [i], S. Miscetti [b], M. Moulson [b], S. Müller [c], F. Murtas [b], M. Napolitano [e], A. Nedosekin [b,o], F. Nguyen [j], M. Palutan [b], E. Pasqualucci [h], L. Passalacqua [b], A. Passeri [j], V. Patera [b,g], F. Perfetto [e], E. Petrolo [h], L. Pontecorvo [h], M. Primavera [d], F. Ruggieri [a], P. Santangelo [b], E. Santovetti [i], G. Saracino [e], R. D. Schamberger [k], B. Sciascia [b], A. Sciubba [b,g], F. Scuri [f], I. Sfiligoi [b], A. Sibidanov [b], T. Spadaro [b], E. Spiriti [j], M. Testa [h], L. Tortora [j], P. Valente [b], B. Valeriani [c], G. Venanzoni [f], S. Veneziano [h], A. Ventura [d], S.Ventura [h], R.Versaci [j], I. Villella [e], G. Xu [b,n]

[1] Corresponding author: M. Incagli, e-mail marco.incagli@pi.infn.it

[a] *Dipartimento di Fisica dell'Università e Sezione INFN, Bari, Italy.*

[b] *Laboratori Nazionali di Frascati dell'INFN, Frascati, Italy.*

[c] *Institut für Experimentelle Kernphysik, Universität Karlsruhe, Germany.*

[d] *Dipartimento di Fisica dell'Università e Sezione INFN, Lecce, Italy.*

[e] *Dipartimento di Scienze Fisiche dell'Università "Federico II" e Sezione INFN, Napoli, Italy*

[f] *Dipartimento di Fisica dell'Università e Sezione INFN, Pisa, Italy.*

[g] *Dipartimento di Energetica dell'Università "La Sapienza", Roma, Italy.*

[h] *Dipartimento di Fisica dell'Università "La Sapienza" e Sezione INFN, Roma, Italy.*

[i] *Dipartimento di Fisica dell'Università "Tor Vergata" e Sezione INFN, Roma, Italy.*

[j] *Dipartimento di Fisica dell'Università "Roma Tre" e Sezione INFN, Roma, Italy.*

[k] *Physics Department, State University of New York at Stony Brook, USA.*

[ℓ] *Dipartimento di Fisica dell'Università e Sezione INFN, Trieste, Italy.*

[m] *Physics Department, University of Virginia, USA.*

[n] *Permanent address: Institute of High Energy Physics, CAS, Beijing, China.*

[o] *Permanent address: Institute for Theoretical and Experimental Physics, Moscow, Russia.*

[p] *Permanent address: High Energy Physics Institute, Tbilisi State University, Tbilisi, Georgia.*

Abstract

We have measured the cross section $\sigma(e^+e^-\to\pi^+\pi^-\gamma)$ with the KLOE detector at DAΦNE, at an energy $W = M_\phi = 1.02$ GeV. From the dependence of the cross section on $m(\pi^+\pi^-) = \sqrt{W^2 - 2WE_\gamma}$, where E_γ is the energy of the photon radiated from the initial state, we extract $\sigma(e^+e^-\to\pi^+\pi^-)$ for the mass range $0.35 < m^2(\pi^+\pi^-) < 0.95$ GeV^2. From our result we extract the pion form factor and the hadronic contribution to the muon anomaly, a_μ.

1 Hadronic Cross Section at DAΦNE

1.1 Motivation

The recent precision measurement of the muon anomaly a_μ at the Brookhaven National Laboratory [1] has led to renewed interest in accurate measure-

ments of the cross section for e^+e^- annihilation into hadrons. Contributions to the photon spectral functions due to quark loops, are not calculable for low hadronic mass states because of the failure of perturbative QCD in such conditions. A very clean way out has been known for a long time [2]. The imaginary part of the hadronic piece of the spectral function is connected by unitarity to the cross section for $e^+e^-\rightarrow$hadrons. A dispersion relation can thus be derived, giving the contribution to a_μ as an integral over the hadronic cross section multiplied by an appropriate kernel. An example of a first complete estimate of the correction was given in 1985, $\delta a_\mu^{\rm had}$=707(6)(17) $\times 10^{-10}$ [3]. The process $e^+e^-\rightarrow\pi^+\pi^-$ contributes $\sim$500 out of the $\sim$700 value above. The cross section for $e^+e^-\rightarrow\pi^+\pi^-$ becomes negligible above 1 GeV.

The most recent measurements of $\sigma(e^+e^-\rightarrow\pi^+\pi^-)$ in the energy interval 610$<$ $m(\pi^+\pi^-)$ $<$961 MeV come from CMD-2 at Novosibirsk. They claim a systematic error of 0.6% with a statistical error of $\sim$0.7% [4]. Their data have been used most recently together with τ and e^+e^- data up to 3 GeV, in an attempt to produce a firm prediction for comparison with the BNL result[5]. There is unfortunately a rather strong disagreement between the $\delta a_\mu^{\rm had}$ value obtained using $e^+e^-\rightarrow\pi^+\pi^-$ data and τ decay data, after isospin corrections. Finally the $e^+e^-\rightarrow\pi^+\pi^-$ based result disagrees by $\sim$3 σ with the BNL [1] measurements. There are thus many reasons for new measurements of the e^+e^- annihilation cross section into two pions.

1.2 Initial State Radiation

Initial state radiation, ISR, is a convenient mechanism which allows studying $e^+e^-\rightarrow$ hadrons, over the entire energy range from $2m_\pi$ to W, the center of mass energy of the collision. In the case of interest it is potentially vitiated by the possibility of final state radiation. For a photon radiated before annihilation of the e^+e^- pair, the $\pi^+\pi^-$ system energy is $m(\pi^+\pi^-) = \sqrt{W^2 - 2WE_\gamma}$, thus one measures the coupling to pions of an off-mass shell photon of mass m($\pi^+\pi^-$). For a photon radiated by the final state pions, the virtual photon coupling to the $\pi^+\pi^-$ pair has a mass W. By just counting powers of α, the relative probability of ISR and FSR are equal. This requires very careful estimates of the two processes in order to be able to use the reaction $e^+e^-\rightarrow\pi^+\pi^-\gamma$ to extract $\sigma(e^+e^-\rightarrow\pi^+\pi^-)$. The Karlsruhe group has given much attention to this problem and has also developed the EVA and PHOKHARA Monte Carlo programs [6] - [10] which are fundamental to our analysis. In the following we will refer to the invariant mass squared of the $\pi^+\pi^-$ system as s_π. In general the $\pi^+\pi^-\gamma$ and $\pi^+\pi^-$ cross section are related through:

$$s_\pi \frac{{\rm d}\sigma(\pi^+\pi^-\gamma)}{{\rm d}s_\pi\, {\rm d}\cos\theta} = \sigma(\pi^+\pi^-,\ s_\pi) \times F(s_\pi,\ \theta_\gamma)$$

Integrating the cross section above, for $0 < \theta_\gamma < \overline{\theta}$ and $180^\circ - \overline{\theta} < \theta_\gamma < 180$ we get

$$s_\pi \frac{\mathrm{d}\sigma(\pi^+\pi^-\gamma)}{\mathrm{d}s_\pi} = \sigma(\pi^+\pi^-,\ s_\pi) \times H(s_\pi,\ \overline{\theta}) \tag{1}$$

Eq. 1 defines the radiator function $H(s_\pi,\ \overline{\theta})$. In the following we will drop the variable $\overline{\theta}$ which is a constant in the present work. The radiator function H used in our analysis is obtained from the PHOKHARA Monte Carlo program. Our present analysis is based on the observation of ref.[6], that for small polar angle of the radiated photon, the ISR process vastly dominates over the FSR process. At lowest order the $\pi^+\pi^-\gamma$ cross section diverges as $1/\sin^2\theta$, just like $\sigma(e^+e^-\to\gamma\gamma)$. We limit ourselves in the following to studying the reaction $e^+e^-\to\pi^+\pi^-\gamma$ with $\theta_\gamma < 15^\circ$ or $\theta_\gamma > 165^\circ$. For small $m(\pi^+\pi^-)$, the di-pion system recoiling against a small angle photon will results in one or both pions being lost also at small angle. We are therefore limited to measuring $\sigma(\pi^+\pi^-)$ for $m(\pi^+\pi^-)$ >550 MeV. We will be able to investigate the cross section near threshold, as soon as next to leading order calculation for FSR become available. This is of great importance, since there are no recent, good measurements of $\sigma(\pi^+\pi^-)$ at low mass, which weigh strongly in the estimate of $\delta a_\mu^{\mathrm{had}}$.

2 The KLOE detector

The KLOE detector [11] consists of only two elements: a large, precision drift chamber and an electromagnetic calorimeter. The detector design was optimized for CP study in neutral kaon decays, for K mesons produced in the decay of ϕ mesons almost at rest, p_ϕ∼12.5 MeV/c. The measurements reported in the following rely heavily on the drift chamber. Its large dimensions, 4 m diameter, use of He and a magnetic field of 0.52 T allow measuring momenta and direction of charged particles with very high accuracy. Because of our choice of accepting only events with $|\cos\theta_\gamma| > \cos 15^\circ$, the photon does not reach the calorimeter. The two relevant parameters, s_π and θ_γ are obtained from the reconstructed tracks of events with two opposite charge particles forming a vertex near the e^+e^- interaction point. The quality of the detector is fully described by the mass squared resolution and the resolution in measuring the production angle of single tracks or the angle of the vector sum of the two track momenta. We find $\sigma(m(\pi^+\pi^-))/m$∼0.2% for m=500 MeV, without much change over the range studied and $\sigma(\theta_\gamma)$∼10 mrad, with $\theta_\gamma = \cos^{-1}(\mathbf{p}_{+-}\cdot\hat{z})$ and $\mathbf{p}_{+-} = -(\mathbf{p}^+ + \mathbf{p}^-)/|(\mathbf{p}^+ + \mathbf{p}^-)|$. The momentum resolution is $\sigma(p_\perp)/p_\perp \le 0.4\%$ for large angle tracks. The calorimeter still plays an important role in the measurement. Its exceptional timing resolution,

$\sigma(t) = 57/\sqrt{E\ \mathrm{GeV}} \oplus 50$ ps and high segmentation provide particle identification allowing us to distinguish pion from electrons and muons, as discussed later. It is also used in the luminosity measurement,

The KLOE detector is operated at DAΦNE, the Frascati ϕ–factory, running at $W = m_\phi = 1019.4$ MeV. Beams cross in DAΦNE at an angle of 25 mrad, resulting in a momentum of the ϕ mesons of $\sim$12.5 MeV/c along the x-axis. We use a coordinate system where the x-axis points to the center of the colliders, the z-axis bisects the two beam lines and the y-axis is vertical. The precise values of W and p_ϕ is measured on a run by run basis using Bhabha events, to accuracies significantly better than 100 keV. The rms machine energy spread is $\sim$350 keV, measured with $K_S K_L$ pairs in KLOE.

3 Event Selection

The excellent KLOE resolution allows us to efficiently selected $\pi^+\pi^-\gamma$ events, without photon detection, because of their clean signature: two tracks from the interaction point. We assume that the event is of the type $e^+e^-\to x^+x^-\gamma$, with $m(x^+) = m(x^-)$ and $m_x = m_\pi$. The undetected photon polar angle, θ_γ is the angle with the z-axis of the vector -$\mathbf{p}_+$-$\mathbf{p}_-$.

3.1 Fiducial Volume

The fiducial volume for $\pi^+\pi^-\gamma$ events has been chosen in order to maximize the acceptance for $\pi^+\pi^-\gamma$ events due to ISR. The main background processes are $e^+e^-\to\phi\to\pi^+\pi^-\pi^0$ and radiative Bhabha scattering. At low mass the final state $\mu^+\mu^-\gamma$ becomes important but requiring small θ_γ removes most of this final state. We rely otherwise on kinematics and particle identification, ID, in order to reject the mentioned backgrounds to a negligible level. From studies with EVA, confirmed with PHOKHARA, a good compromise for the fiducial volume is $|\cos\theta_\gamma| > \cos 15^\circ$ and $50^\circ < \theta_{+-} < 130$ for the polar angle of both tracks at the interaction point. These requirements ensure abundant statistics for the measurement and contamination of FSR hard radiation well below the 1% level. The efficiency for the events falling inside the fiducial cuts is contained in the value of the radiator, obtained from PHOKHARA. We note that no detected photon is required, nor are events rejected if photons are present.

3.2 Event Selection

3.2.1 Event origin

The two tracks must form a vertex close to the interaction point. We require that the vertex coordinates x_V, x_y, x_z satisfy $\sqrt{x_V^2 + y_V^2} \leq 8$ cm and $|z_V| \leq 7$ cm. We also require $P_\perp > 160$ or $P_z > 90$ MeV/c to remove spiraling tracks. 90 to 95% of the $\pi^+\pi^-\gamma$ events survive these requirements. This result is obtained from Monte Carlo studies and examination of $\phi \to \pi^+\pi^-$ decays.

3.2.2 Pion identification

A fraction of radiative Bhabha events, $e^+e^-\gamma$, survives kinematical selection, see sec. 3.2.3 below, contributing a non-negligible background. In order to reject these events, we have developed a particle ID method, using approximate likelihood estimators which are effective in distinguishing pion and electrons. The likelihood is based on time-of-flight vs momentum comparison and on the shape and magnitude of the energy deposits in the calorimeter by the charged particles. Correlations, which are significant, between used variables are ignored. Two likelihood functions have been built using actual data: one, L_π to test the pion hypothesis [2] (using $\pi^+\pi^-\pi^0$ events) and the other, L_e to test the electron hypothesis (using Bhabha events). We require that candidate pion tracks have a greater likelihood of being pions than of being electrons. We use as discriminating variable $\zeta = \log(L_\pi/L_e)$ and we accept as pions particles with $\zeta > 0$, see fig. 1. The efficiency for pions is $\sim$98% and 3% of the electrons survive rejection. We require that only one of the two particles satisfy the pion ID requirement (OR) achieving an efficiency of 100% with some very small residual background. Requiring that both tracks are pions (AND) leads to a 5% loss. We use the AND for evaluating backgrounds, see later.

3.2.3 Kinematic Cuts

For an $x^+x^-\gamma$ final state Lorentz invariance allows us to compute the mass of x, which we call $m_{\rm trk}$ from

$$\left(M_\phi - \sqrt{\mathbf{p}_+^2 + m_{\rm trk}^2} - \sqrt{\mathbf{p}_-^2 + m_{\rm trk}^2}\right)^2 - (\mathbf{p}_+ + \mathbf{p}_-)^2 = 0 \qquad (2)$$

[2] In fact, in the case of the pion likelihood, two different functions are built, one for π^+ and one for π^-, since the energy deposition of the two particles is different, in particular at these energies. This is not necessary for electrons.

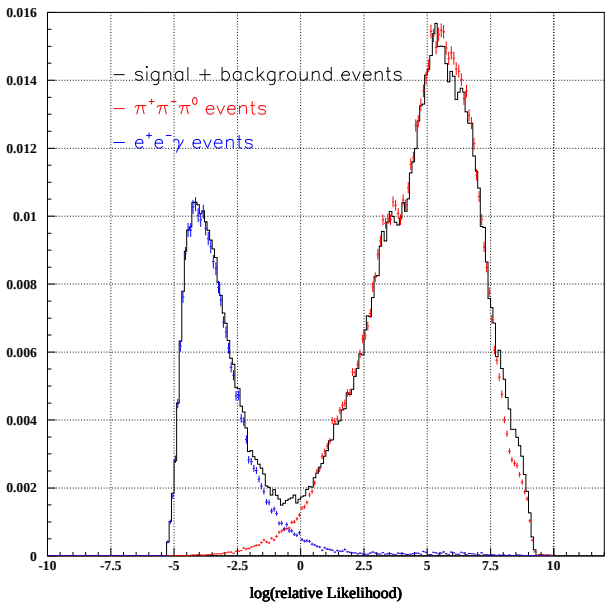

Fig. 1. Distribution of the particle ID variable ζ for pions, right peak, and electrons, left. See text.

For $e^+e^- \to x^+x^-\gamma$, the value of $m_{\rm trk}$ peaks at m_π, m_μ, m_e thus allowing selection of signal events. The density distribution of the two track events in the $[s_\pi,\ m_{\rm trk}]$ plane is very effective for separating signal from background. The distribution is shown in fig. 2 together with the selection cut defined by: $(m_{\rm trk} > 120) \odot (m_{\rm trk} < 250 - 105\sqrt{1 - s_\pi/0.85^2}) \odot (m_{\rm trk} < 220)$, all units in MeV. $\pi^+\pi^-\pi^0$ events populate a curve in the plane. The signal events above the region $m_{\rm trk} > 140$ MeV are due to additional ISR or FSR radiation. The cut on $m_{\rm trk}$ rejects a fraction of events with additional radiation. The implications are discussed in section 4.4.

4 Event Analysis

Data were taken in July through December 2001, for an integrated luminosity of Ł=140.7 pb^{-1}. After fiducial volume and selection cuts we find $\sim$1.5 $\times$ 10^6 events. Fig. 3 gives the $\pi^+\pi^-$ mass squared distribution of the $\pi^+\pi^-\gamma$ events in bins of 0.01 GeV^{-2} in s_π. The ρ peak and the ρ-ω interference structure are clearly visible, demonstrating the excellent mass resolution of the KLOE detector. To obtain the cross section, we subtract the residual background from this spectrum and divide by the selection efficiency and the integrated luminosity:

$$\frac{\Delta\sigma_{\pi^+\pi^-\gamma}}{\Delta s_\pi} = \frac{\Delta N_{\pi^+\pi^-\gamma}}{\text{Ł}\ \Delta s_\pi} = \frac{\Delta N_{\rm obs} - \Delta N_{\rm bckgnd}}{\text{Ł}\ \Delta s_\pi} \times \frac{1}{\epsilon_{\rm cuts}} \qquad (3)$$

4.1 Background

The $[s_\pi,\ m_{\rm trk}]$ plane population of signal and background events is illustrated in fig. 2. The amount of background in the signal region is obtained by fitting the $m_{\rm trk}$ spectrum of the selected events, in slices of s_π with the $m_{\rm trk}$ spectra for signal, $e^+e^-\gamma$ and $\mu^+\mu^-\gamma$ events obtained from Monte Carlo simulation. An example of such a fit is shown in fig. 4, left. Background from $\pi^+\pi^-\pi^0$ events appears at higher $m_{\rm trk}$ values and the missing mass, $m^2_{miss} = (p_\phi - p_+ - p_-)^2$, peaks at $m(\pi^0)$. The $\pi^+\pi^-\pi^0$ background count is obtained by fitting the $m_{\rm miss}$ distribution with the shapes obtained from the Monte Carlo simulation. An example of such a fit is shown in fig. 4, right. The result of the fits is shown in fig. 5 which shows the relative contribution of the different backgrounds to the observed signal. The shape of the background distribution is well reproduced by the Monte Carlo simulation ensuring that systematic uncertainties are smaller than the fit errors. Other possible contributions, such as the reaction $e^+e^-\to e^+e^-\pi^+\pi^-$ with the electrons going down the beam pipe, have been studied and shown to be negligible given our event selection criteria.

4.2 Luminosity Measurement

The integrated luminosity is measured using large angle Bhabha (LAB) events, with the KLOE detector itself. The effective Bhabha cross section at large angles ($55^o < \theta_{+,-} < 125^o$) is about 430 nb. This cross section is large enough

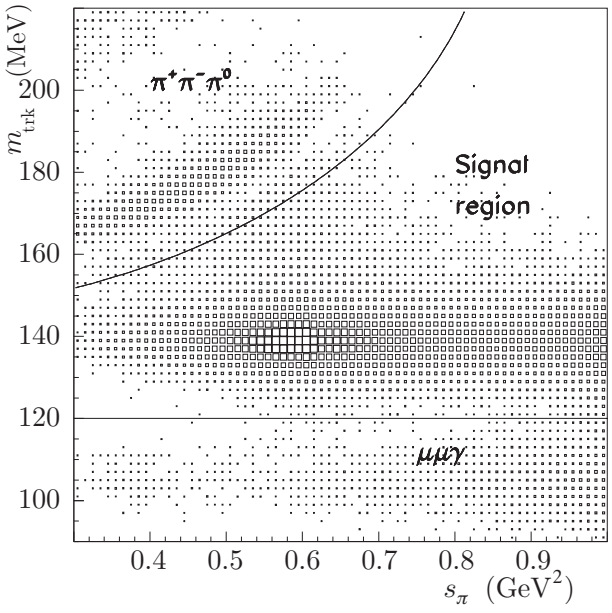

Fig. 2. Kinematic separation, in the $[m_{\rm trk}, s_\pi]$ plane, of signal and backgrounds after the ζ variable cut.

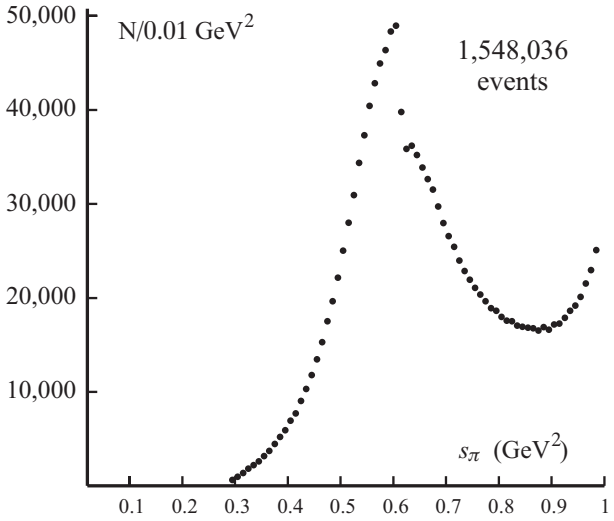

Fig. 3. Events per 0.01 GeV^2 after fiducial volume and selection cuts.

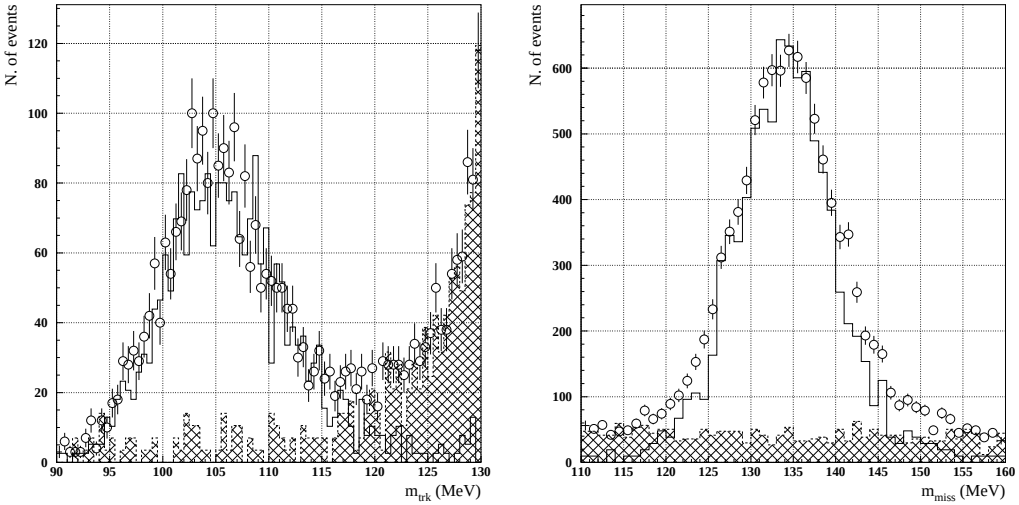

Fig. 4. Muon mass fit, left and π^0 mass fit, right. These fits are used to estimate the $\mu^+\mu^-\gamma$ and $\pi^+\pi^-\pi^0$ backgrounds (shaded areas) to the $\pi^+\pi^-\gamma$ channel.

so that the statistical error on the luminosity measurement is negligible. The number of LAB candidates, N_{LAB}, is counted and normalized to the effective Bhabha cross section, obtained by Monte Carlo:

$$\int \mathcal{L}dt = \frac{N_{LAB}(\theta_i)}{\sigma^{MC}_{LAB}(\theta_i)} \cdot (1 - \delta_{Bkg}) \tag{4}$$

The precision of this measurement depends on the correct inclusion of higher order terms in computing the Bhabha cross section. We use two independent Bhabha event generators: BHAGENF ([14], [15]) and BABAYAGA ([16]). For

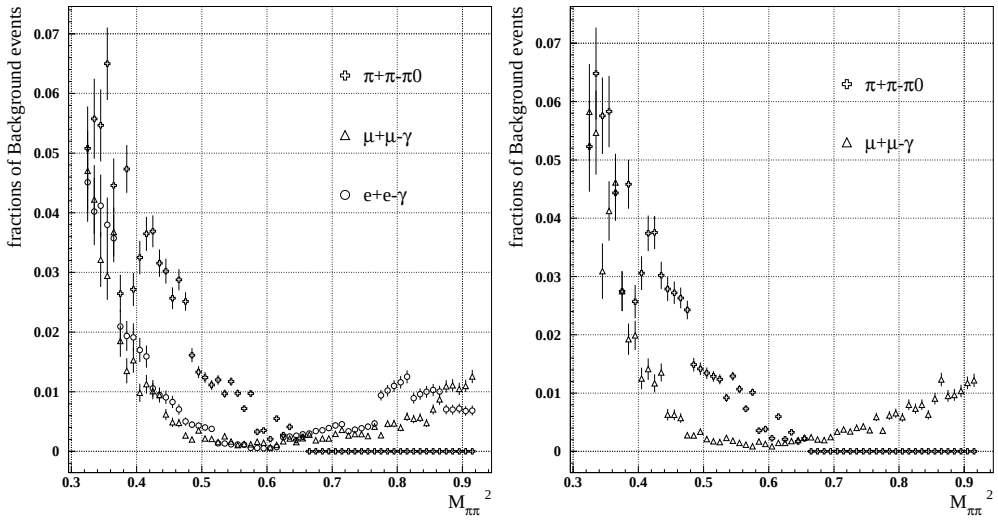

Fig. 5. Left: backgrounds fractions requiring a single identified pion (OR) and right: two identified pions (AND) which removes completely the residual Bhabhas.

each generator a systematic error of 0.5% is quoted by the authors. The two result for the luminosity agree to better than 0.2%.

LAB events are selected with cuts on variables which are well simulated by the KLOE Monte Carlo simulation. The electron and positron polar angle cuts, $55^\circ < \theta_{+,-} < 125^\circ$, is based on the calorimeter clusters, while the energy cuts, $E_{+,-} > 400$ MeV, is based on drift chamber information. The background from $\mu^+\mu^-(\gamma)$, $\pi^+\pi^-(\gamma)$ and $\pi^+\pi^-\pi^0$ events is well below 1% and is subtracted. All selection efficiencies (trigger, EmC cluster, DC tracking) are $> 99\%$ and are well reproduced by the detector simulation program. We also obtain excellent agreement between the experimental distributions ($\theta_{+,-}$, $E_{+,-}$) and those obtained from Monte Carlo simulation, see fig. 6. Finally, corrections are applied on a run-by-run basis for fluctuations in the center-of-mass energy of the machine and in the detector calibrations. The experimental uncertainty in the acceptance due to all these effects is 0.4%. We assign a total systematic error for the luminosity of $\delta\mathrm{L} = 0.5\%_{\mathrm{th}} \oplus 0.4\%_{\mathrm{exp}}$. An independent check of the luminosity measurement is obtained using $e^+e^- \to \gamma\gamma$ events. We find agreement to within 0.2%.

4.3 Selection Efficiencies

4.3.1 Trigger, tracking and vertexing

These efficiencies have been obtained from control samples of $\pi^+\pi^-\pi^0$, $\pi^+\pi^-$ and $\pi^+\pi^-\gamma$ events selected without requiring the vertex. The efficiencies have been parameterized as a function of single track parameters (charge, momentum and angle) combined using Monte Carlo simulation. The largest source

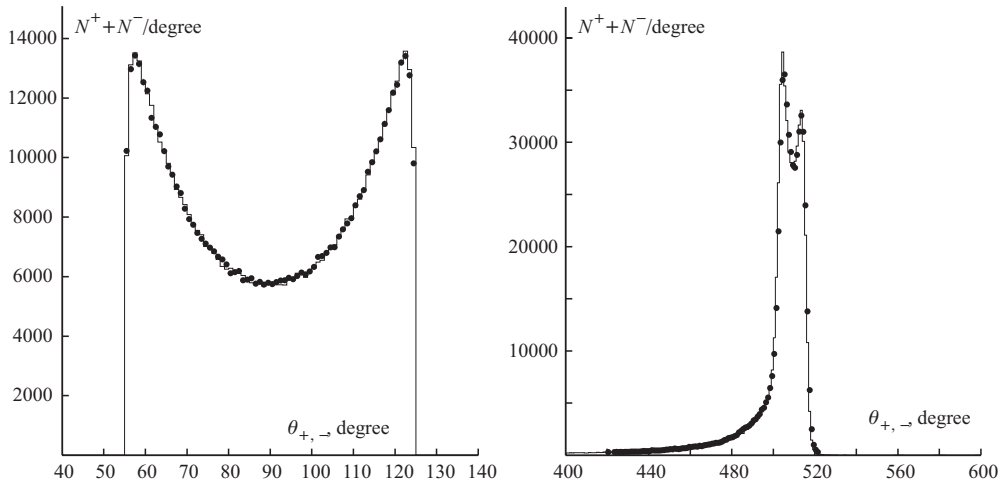

Fig. 6. Comparison data-Monte Carlo of the $\theta_{+,-}$ (left) and $E_{+,-}$ (right) distributions for the Bhabha events selected at large angle as described in the text.

of systematic error in this procedure arises from the difference between the kinematics of the control samples and the signal.

4.3.2 Pion identification

. The efficiency for the ζ cut has been evaluated from data by accepting one track and studying the distribution of the other one. The systematic error introduced by the ζ cut is negligible, since we use the OR, *i.e.* at least on particle is a pion, for which the efficiency is $\sim$100% for $\pi^+\pi^-\gamma$ events.

4.3.3 Particle mass

The efficiency for the $m_{\rm trk}$ cut is obtained as a by-product of the residual background evaluation; the result of the fit provides the efficiency in each s_π bin. However, this efficiency depends upon the way the Monte Carlo simulation treats multi-photon processes. The $m_{\rm trk}$ efficiency has been obtained with our reference Monte Carlo simulation, which uses the PHOKHARA version 1.0 generator. PHOKHARA simulates the full NLO QED correction for e^+e^- annihilation with the emission of additional photons from the initial state. In order to estimate the systematic effect due to the generator we have repeated the exercise using a different generator, BABAYAGA ver.3.5, the same generator used in the luminosity measurement. In this generator, ISR is treated using the parton shower approach. The resulting value for the $m_{\rm trk}$ efficiency differs from that evaluated with PHOKHARA by 0.2%. An additional contribution, which is treated separately, is the emission of both an ISR and FSR photon. This is discussed in the next section. The contribution of the systematic error for each efficiency to the total error is shown in table 1.

Acceptance	0.3%
Trigger	0.6%
Tracking	0.3%
Vertex	1.0 %
Likelihood	0.1 %
Track Mass	0.2 %
Background subtraction	0.5 %
Unfolding	0.6 %
Total exp systematics	1.4 %
luminosity	0.6 %
Vacuum Polarization	0.2 %
Total theor. systematics	0.7 %
FSR resummation	2.0 %

Table 1
List of systematic uncertainties from the three sources: experimental, theoretical and ignoring FSR.

4.4 Unfolding the mass resolution

In order to obtain $\mathrm{d}\sigma_{\pi\pi\gamma}/\mathrm{d}s_\pi$ as a function of the true s_π value, we unfold the mass resolution from the measured s_π distribution. The measured value of $s_{\pi,\mathrm{obs}}$ is related to the true value by a resolution matrix $\mathbf{G}(s_{\pi,\mathrm{true}} - s_{\pi,\mathrm{obs}}|s_{\pi,\mathrm{true}})$. This matrix has been generated by Monte Carlo simulation. The resolution matrix is nearly diagonal with 75% of the events in the diagonal, 11% in each of the first once-off-diagonal elements and only 3% in the remaining elements. The matrix is graphically illustrated in fig. 7, left. Unfolding is obtained by applying the inverse matrix $\mathbf{G}^{-1}$ to the data. The result is shown in fig. 7, right, which shows the difference between the reconstructed and the generated spectra with and without the application of the unfolding procedure. This procedure does not affect the value of a_μ, since the correlation is short range, $\simeq 97\%$ of the events being in the same or the adjacent bins.

5 Results

The cross section for $e^+e^- \to \pi^+\pi^-\gamma$, after applying the corrections described above, is shown in fig. 8. In order to get the $e^+e^- \to \pi^+\pi^-$ cross section, the radiator function $H(s_\pi, \overline{\theta}_\gamma)$ is needed. The radiator is obtained from PHOKHARA, setting $F_\pi(s_\pi) = 1$ and *switching off* the vacuum polarization of the intermediate photon in the generator. The radiator $H(s_\pi, \overline{\theta}_\gamma = 15^\circ)$ is also shown in fig.8, left.

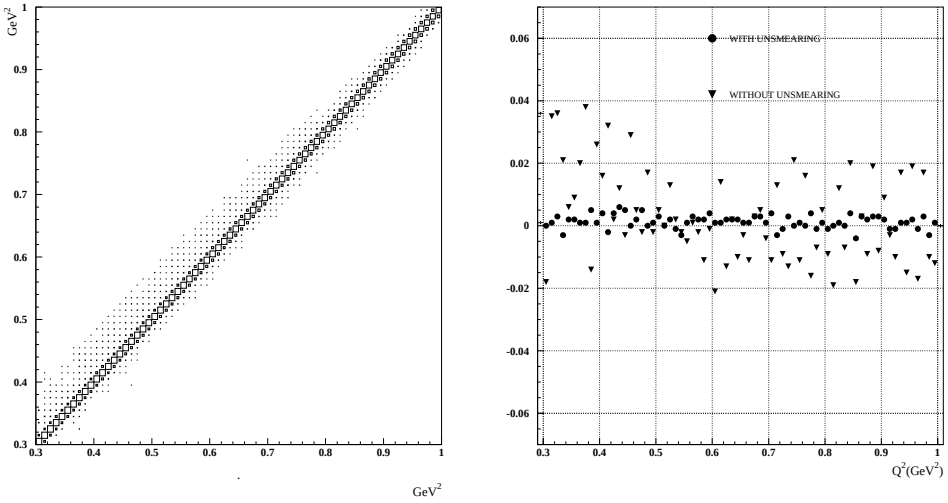

Fig. 7. Left: smearing matrix representing the correlation between generated and reconstructed s_π value; the high precision of the DC results in an almost diagonal matrix. Right: fractional difference between reconstructed and generated spectrum with and without resolution unfolding.

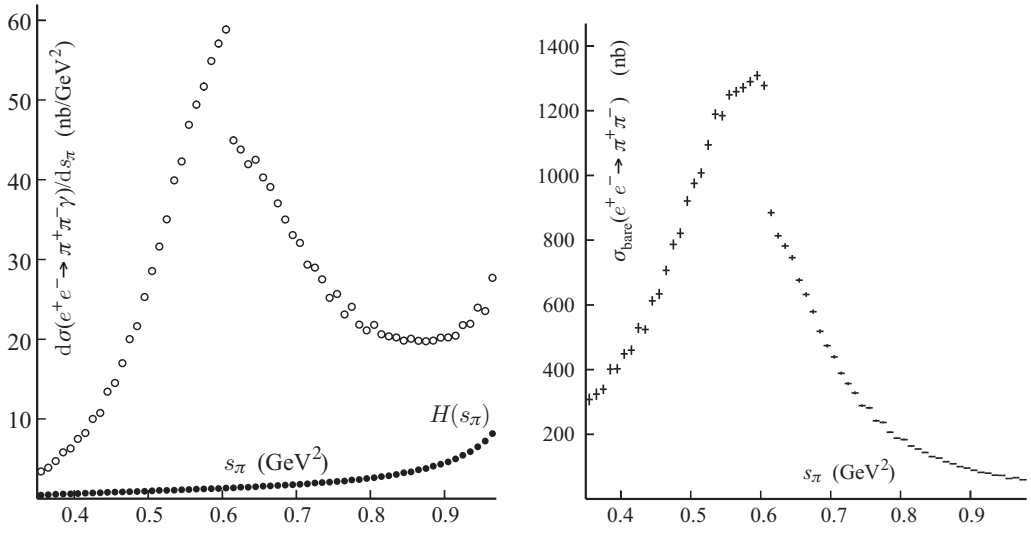

Fig. 8. Left. Cross section for $e^+e^- \to \pi^+\pi^-\gamma$. The radiator $H(s_\pi, \overline{\theta}_\gamma)$, is also shown. Right. *Bare* cross section for $e^+e^- \to \pi^+\pi^-$.

5.1 FSR and Vacuum Polarization corrections

Part of the multiphoton events are removed by the m_{trk} cut. The effect of this cut is evaluated using PHOKHARA 1.0 which, however, does not include soft radiation in the final state accompanying one hard photon from the initial state. An preliminary estimate done with PHOKHARA-II, shows that this effect is smaller than 2%. We *do not correct* here for FSR photons and we

include in the theoretical systematic error the full value (2%) due to this effect. In order to obtain the pion form factor, or the *bare* cross section, vacuum polarization effects must be subtracted. This can be done by correcting the cross section for the running of α, see refs. [17], [5], as follows:

$$\sigma_{\rm bare} = \sigma_{\rm dressed} \left(\frac{\alpha(0)}{\alpha(s)} \right)^2 \tag{5}$$

We have used an approximate, but quite adequate for the purpose estimate of $\alpha(s)$[18]. Fig. 8, right, shows the resulting cross section.

5.2 Results and comparisons with existing data

We have used the *bare* cross section to evaluate of $\delta a_\mu^{\rm had}$ in the region covered by the CMD-2 experiment ($0.37 < s_\pi < 0.93$). The resulting value (in 10^{-10} units) is :

$$\delta a_\mu^{\rm had} = 374.1 \pm 1.1_{\rm stat} \pm 5.2_{\rm syst} \pm 2.6_{\rm theo} \ {}^{+7.5}_{-0.0}\Big|_{\rm FSR} \tag{6}$$

to be compared with:

$$\delta a_\mu^{\rm had}({\rm CMD\text{-}2}) = 368.1 \pm 2.6_{\rm stat} \pm 2.2_{\rm syst+theo} \tag{7}$$

The statistical error is negligible. The systematic error is at the moment at the 1.4% value, but there is still room to improve it down to $\simeq 1\%$. Clearly the dominating error is the one we have conservatively assigned to the FSR radiation effect. This error will be substantially reduced once the new PHOKHARA version will be inserted into the KLOE MC.

The central value of our result in the region $0.37 < s_\pi < 0.93$ is slightly larger than the one obtained by CMD-2. The discrepancy is, at the moment, not significant (0.5 σ). This difference is, however, not equally distributed in s_π, as summarized below. [3]

s_π, GeV^2	δa_μ, KLOE	δa_μ, CMD-2
0.37 – 0.60	$256.2 \pm 4.1 (^{+5.1}_{-0}$ FSR)	249.7 ± 2.2
0.60 – 0.93	$117.9 \pm 2.1 (^{+2.3}_{-0}$ FSR)	119.8 ± 1.1

Our data differ from the CMD-2 results mostly below the ρ-peak. However, for the mass squared range $0.6 < s_\pi < 0.9$, our data confirm the discrepancy between τ data and $e^+e^- \to \pi^+\pi^-$ results, which is $\sim$10-15%.

[3] This is our evaluation of $a_\mu^{\rm had}$(CMD-2), based on the values tabulated in ref. [4]

Acknowledgements

We thank the DAΦNE team for their efforts in maintaining low background running conditions and their collaboration during all data-taking. We want to thank our technical staff: G. F. Fortugno for his dedicated work to ensure an efficient operation of the KLOE Computing Center; M. Anelli for his continous support to the gas system and the safety of the detector; A. Balla, M. Gatta, G. Corradi and G. Papalino for the maintenance of the electronics; M. Santoni, G. Paoluzzi and R. Rosellini for the general support to the detector; C. Pinto (Bari), C. Pinto (Lecce), C. Piscitelli and A. Rossi for their help during shutdown periods. This work was supported in part by DOE grant DE-FG-02-97ER41027; by EURODAPHNE, contract FMRX-CT98-0169; by the German Federal Ministry of Education and Research (BMBF) contract 06-KA-957; by Graduiertenkolleg 'H.E. Phys. and Part. Astrophys.' of Deutsche Forschungsgemeinschaft, Contract No. GK 742; by INTAS, contracts 96-624, 99-37; and by TARI, contract HPRI-CT-1999-00088.

References

[1] G.W. Bennet, et al., Phys. Rev. Lett. 89, (2002) 101. See also references 1-4 in this paper.

[2] L. Durand, Phys. Rev. **128**, 441 (1962); M. Gourdin and E. de Rafael, Nucl. Phys. **B10**, 667 (1696)

[3] T. Kinoshita, B. Nižić and Y. Okamoto, Phys. Rev. D **31**, 2108 (1985)

[4] R.R. Akhmetshin et al. The data were taken in 1994-95 and first presented in hep-ex/9904027. R.R. Akhmetshin et al. Phys. Lett. B 476 (2000) 33; Phys. Let. B 527 (2002) 161-172

[5] M. Davier, S. Eidelman, A. Höcker and Z. Zhang, Eur. Phys. J. C 27, (2003) 497, hep-ph/0208177

[6] S. Binner, J.H. Kühn, K. Melnikov, Phys.Lett. B **459** (1999) 279

[7] G. Rodrigo, A. Gehrmann-De Ridder, M. Guilleaume, J.H. Kühn, Eur. Phys. J. C **22**, 81 (2001);

[8] G. Rodrigo, H. Czyz, J.H. Kühn and M. Szopa, Eur. Phys. J C **24** (2002) 71

[9] H. Czyz, A. Grzelinska, J. H. Kühn and G. Rodrigo, Eur. Phys. J. C **27**, 563 (2003).)

[10] K. Melnikov, F, Nguyen, B. Valeriani, G. Venanzoni, Phys. Lett. B477, (2000) 114

[11] A. Aloisio *et al.* [KLOE collaboration], *The KLOE Detetor, Technical Proposal*, **LNF-93/002** (1993)

[12] M. Adinolfi *et al.* [KLOE collaboration], *The Tracking Detector of the KLOE Experiment*, **LNF-01/016** (2001); to be published in Nuclear Instruments and Methods

[13] M. Adinolfi *et al.* [KLOE collaboration], *The KLOE electromagnetic calorimeter*, **LNF-01/017** (2001); to be published in Nuclear Instruments and Methods

[14] F.A. Berends, R. Kleiss, Nucl.Phys. B **228** (1988) 537

[15] E. Drago, G. Venanzoni, *A Bhabha Generator for DAΦNE including radiative corrections and ϕ resonance*, **INFN/AE-97/48** (1997)

[16] C.M.C. Calame, C. Lunardini, G. Montagna, O. Nicrosini, F. Piccinini, Nucl.Phys. B **584** (2000) 459

[17] A. Höfer, J. Gluza and F. Jegerlehner, Eur. Phys. J C **24** (2002) 51

[18] We thank F. Jegerlehner for kindly providing a table of $\Delta\alpha_{\rm hadr}(s)$ values. The leptonic contribution is obtained analytically.